

ANTIFAKEPROMPT: PROMPT-TUNED VISION-LANGUAGE MODELS ARE FAKE IMAGE DETECTORS

You-Ming Chang^{1*} Chen Yeh^{1*} Wei-Chen Chiu¹ Ning Yu²

¹National Yang Ming Chiao Tung University ²Salesforce Research
{thisismiiiiing.11, denny3388.cs11}@nycu.edu.tw
walon@nctu.edu.tw, ning.yu@salesforce.com

ABSTRACT

Deep generative models can create remarkably photorealistic fake images while raising concerns about misinformation and copyright infringement, known as deepfake threats. Deepfake detection technique is developed to distinguish between real and fake images, where the existing methods typically train classifiers in the image domain or various feature domains. However, the generalizability of deepfake detection against emerging and more advanced generative models remains challenging. In this paper, inspired by the zero-shot advantages of Vision-Language Models (VLMs), we propose a novel approach using VLMs (e.g. InstructBLIP) and prompt tuning techniques to improve the deepfake detection accuracy over unseen data. We formulate deepfake detection as a visual question answering problem, and tune soft prompts for InstructBLIP to distinguish a query image is real or fake. We conduct full-spectrum experiments on datasets from 3 held-in and 13 held-out generative models, covering modern text-to-image generation, image editing and image attacks. Results demonstrate that (1) the deepfake detection accuracy can be significantly and consistently improved (from 54.6% to 91.31%, in average accuracy over unseen data) using pretrained vision-language models with prompt tuning; (2) our superior performance is at less cost of trainable parameters, resulting in an effective and efficient solution for deepfake detection. Code and models can be found at <https://github.com/nctu-eva-lab/AntifakePrompt>.

1 INTRODUCTION

In recent years, we have witnessed the magic leap upon the development of generative models, where the cutting-edge models such as Stable Diffusion (SD) (Rombach et al., 2022), DALL-E-2 (Ramesh et al., 2022), Imagen (Saharia et al., 2022) and DALL-E-3 (OpenAI, 2023) have become capable of producing high-quality images, ranging from beautiful artworks to incredibly realistic images. However, the progress of such image synthesis technique, which is called "deepfake", poses real threats to our society, as some realistic fake images could be produced to deceive people and spread false information. For example, images of the war in Ukraine could be generated with false or misleading information and may be used for propaganda¹. More concerningly, some of these created images may be falsely claimed as works of photographers or artists, potentially leading to copyright infringements and their misuse in commercial contexts. As BBC reported, some fake artworks generated by text-to-image generation models won first place in an art competition, which harms the fairness of the contest². To protect against these threats arising from deepfake content, the use of effective deepfake detection techniques becomes crucial.

One straightforward deepfake detection prototype is to train a classifier to distinguish between real and fake images (Wang et al., 2020; Guarnera et al., 2023; Yu et al., 2019). However, along with the rapid development of generative models, this approach often struggles with overfitting thus leading

*Both authors contribute equally

¹<https://techcrunch.com/2022/08/12/a-startup-wants-to-democratize-the-tech-behind-dall-e-2-consequences-be-damned/>

²<https://www.bbc.com/news/technology-62788725>

to poor performance on unseen data. To overcome this limitation, researchers are exploring more general features in deepfake images, such as frequency maps of the images (Zhang et al., 2019b). Additionally, some innovative methods are not only based on visual features. For example, DE-FAKE (Sha et al., 2022) harnesses the power of large language models and trains a classifier that conditions on both visual and textual information.

Despite years of development in deepfake detection techniques, challenges persist. First, most previous works such as (Wang et al., 2020) have concentrated on Generative Adversarial Networks (GANs), which may not effectively address the latest diffusion-based generative models, including Stable Diffusion 2 (SD2) (Rombach et al., 2022), Stable Diffusion-XL (SDXL) (Podell et al., 2023), DALLÉ-2 (Ramesh et al., 2022), Imagen (Saharia et al., 2022), and DeepFloyd IF (StabilityAI, 2023). Second, generalizability remains a significant challenge. Classifiers trained on images generated by one model tend to perform poorly when being tested on images from different generative models, especially from more emerging and advanced ones.

To address the aforementioned challenges, we propose a novel deepfake detection method, AntifakePrompt. We have harnessed the zero-shot capabilities of pretrained vision-language models (VLMs) (Li et al., 2022; 2023; Zhu et al., 2023; Liu et al., 2023a; Dai et al., 2023) to capture more general instruction-aware features from images, enhancing the transferability of AntifakePrompt. We formulate the deepfake detection problem as a Visual Question Answering (VQA) task, asking the model with the question "Is this photo real?", to tackle this challenge. However, directly asking questions for a pretrained VLM may not lead to effective answers, considering either the query images or questions are unseen during VLM training. We therefore use prompt tuning to boost the performance. Without loss of generality, we build implementation on the recent state-of-the-art VLM, InstructBLIP (Dai et al., 2023). Specifically, we insert a "pseudo-word" into the prompt and optimize the corresponding word embedding in the model for correctly answering "Yes" and "No" to the question for real and fake images on training data, respectively. This approach not only significantly reduces training costs but also substantially improves performance on both held-in and held-out testing datasets from a full spectrum of generative models. From the perspective of instruction tuning, we realized that there are many good answers, all waiting for a good question. In summary, our paper makes the following key contributions:

1. We pioneer to leverage pretrained vision-language models to solve the deepfake detection problem. We are the first to formulate the problem as a VQA scenario, asking the model to distinguish between real and fake images. Additionally, we employ soft prompt tuning techniques to optimize for the most effective question to the VLMs, and leverage their zero-shot generalizability on unseen data produced by held-out generative models.
2. AntifakePrompt, which is only trained on images from MS COCO and those generated by SD2, consistently outperforms (from 54.6% to 91.31%, in average accuracy over unseen data) the recent baseline methods proposed in (Wang et al., 2020; Sha et al., 2022; Wang et al., 2023) over held-out datasets generated by a full spectrum of generator categories. Our superior performance and generalizability benefit from the nature of pretrained VLMs, and at less cost of trainable parameters.

2 RELATED WORK

2.1 VISUAL GENERATIVE MODELS

The recent advance of deep generative models can be broadly categorized into two main types: Generative-Adversarial-Networks-based (GAN-based) models and diffusion-based models. Within the realm of GAN-based model, notable progress has been made. Starting from GAN (Goodfellow et al., 2014), SA-GAN (Zhang et al., 2019a) and BigGAN (Brock et al., 2018) contributed to the enhancement of training stability and the generation of diverse images with higher resolution. Subsequently, StyleGAN (Karras et al., 2019) and its successors (Karras et al., 2020; 2021) have allowed for finer control over the stylistic attributes of the generated images while maintaining high image quality. Building upon StyleGAN-3 (Karras et al., 2021) and ProjectGAN (Sauer et al., 2021), StyleGAN-XL (SGXL) (Sauer et al., 2022b) is able to generate 1024×1024 images with even lower Fréchet Inception Distance (FID) (Dowson & Landau, 1982) scores and higher Inception Scores (IS) (Salimans et al., 2016), w.r.t. all its predecessors.

In regard to the diffusion-based models, starting from DDPM (Ho et al., 2020), DDIM (Song et al., 2020) speeds up the generating process by relaxing the constraint of Markov Chain towards forward and backward processes. Latent Diffusion (Rombach et al., 2021) and Stable Diffusion (Rombach et al., 2022) further shift the diffusion process to latent space, granting user controls over the models; thus, it flexibly enables the text-to-image generation through diffusion-based models. Afterwards, several successors (e.g. SDXL (Podell et al., 2023), DeepFloyd IF (StabilityAI, 2023), Imagen (Saharia et al., 2022), DALLE-2 (Ramesh et al., 2022), and DALLE-3 (OpenAI, 2023)) further refine the text comprehension capabilities of diffusion-based models, enabling them to create images that better align with input texts.

Apart from text-to-image generation, image editing tasks, such as inpainting and super resolution, are also widely-used applications of generative models. Notably, (Suvorov et al., 2022; Rombach et al., 2022; Liu et al., 2020) have demonstrated exceptional performances in the domain of image inpainting, while (Lee & Jin, 2022; Rombach et al., 2022; Chen et al., 2021) are known for their remarkable performances in image super resolution.

Without the loss of representativeness, we select a diverse set of generative models (namely SD2 (Rombach et al., 2022), SDXL (Podell et al., 2023), IF (StabilityAI, 2023), Dalle-2 (Ramesh et al., 2022), SGXL (Sauer et al., 2022b), ControlNet (Zhang & Agrawala, 2023), LaMa (Suvorov et al., 2022), LTE (Lee & Jin, 2022), SD2-Inpainting model (Rombach et al., 2022), and SD2-SuperResolution model (Rombach et al., 2022)) to cover the full spectrum of generation tasks, and generate corresponding fake images for conducting our experiments.

2.2 DEEPPFAKE DETECTION METHODS

Recent advances in detection methods have focused on training detectors capable of identifying artifacts specific to certain types of generative models. For example, (Wang et al., 2020; Yu et al., 2019) have concentrated on the development of detectors trained upon original or processed features from images generated by GANs, and (Nataraj et al., 2019) employs the co-occurrence matrices directly computed on image pixels on each of red, green and blue channels. (Ricker et al., 2022) finetunes the detector from (Wang et al., 2020) with images generated from additional diffusion-based models and GAN-base models, aiming to exhaust all the latest generative models to achieve better performance. Build upon the idea from (Wang et al., 2020), (Epstein et al., 2023) proposes a detector that can identify generated pixels using a ResNet-50 network trained on datasets with CutMix (Yun et al., 2019) augmentation. While (Sha et al., 2022) uses the coverage difference between prompts and corresponding real or fake images to distinguish real and fake images, (Wang et al., 2023) calculates the reconstruction errors of real and fake images both before and after the diffuse and denoise process. (He et al., 2021) focuses on the structural artifacts with downsampled images as features for image detection.

Further contributions have ventured into artifacts in the frequency domain, such as (Liu et al., 2022; Frank et al., 2020). (Zhang et al., 2019b) proposes AutoGAN that simulates the frequency artifact caused by the pipeline shared by many GAN-base generative models and trains a detector on the spectrum of images generated by AutoGAN. (Giudice et al., 2021) analyses artifacts on images divided by 8x8 blocks and transformed by Discrete Cosine Transform (DCT). (Guo et al., 2023) propose a multi-branch feature extractor that leverages artifacts in both RGB and frequency domain to conduct different levels of classifications, including real/fake and corresponding forgery methods.

These methods have reported outstanding performance on images generated by the models they were designed for, but they often suffer from significant drops in performance when being applied to unseen datasets. Therefore, we aim to propose a general detector that can demonstrate exceptional performance on both in-domain and out-of-domain datasets.

2.3 VISION-LANGUAGE MODELS AND VISUAL QUESTION ANSWERING

With the impressive success of Large language models (LLM) (Chung et al., 2022; Touvron et al., 2023), recent studies work on Vision-Language Models (VLMs) (Li et al., 2022; 2023; Zhu et al., 2023; Liu et al., 2023a; Ye et al., 2023; Dai et al., 2023) to improve multimodal comprehension and generation through utilizing the strong generality of LLMs. These models takes advantage of cross-modal transfer, allowing knowledge to be shared between language and multimodal domains.

BLIP-2 (Li et al., 2023) employing a Flan-T5 (Chung et al., 2022) with a Q-former to efficiently align the visual features with language model. MiniGPT-4 (Zhu et al., 2023) employs the pretrained visual encoder and Q-Former as used in BLIP-2, but chooses Vicuna (Chiang et al., 2023) as the LLM and performs training using ChatGPT³-generated image captions instead of the BLIP-2 training data. InstructBLIP (Dai et al., 2023) also utilizes the pretrained visual encoder and Q-former from BLIP-2, with Vicuna/Flan-T5 as pretrained LLM, but performs instruction tuning on Q-former using a variety of vision-language tasks and datasets. LLaVA (Liu et al., 2023a) projects the output of a visual encoder as input to a LLaMA/Vinuca LLM with a linear layer, and finetunes the LLM on vision-language conversational data generated by GPT-4 (OpenAI, 2023) and ChatGPT. mPLUG-owl (Ye et al., 2023) finetunes a low-rank adaption (Hu et al., 2021) module on a LLaMA (Touvron et al., 2023) model using both text instruction data and vision-language instruction data from LLaVA.

Among the vision-language tasks, visual question answering (VQA) problem is one of the most general and practical tasks because of its flexibility in terms of the questions. For training the models for VQA problems, lots of datasets have been proposed. VQAv2 (Goyal et al., 2017) and VizWiz (Gurari et al., 2018) collect images, questions, as well as the corresponding answers for studying visual understanding. OKVQA (Marino et al., 2019) and A-OKVQA (Schwenk et al., 2022) propose visual question-answer pairs with external knowledge (e.g. Wikipedia). OCR-VQA (Mishra et al., 2019) and TextVQA (Singh et al., 2019) introduce images and questions that require reasoning about text to answer. To solve the VQA problem, TextVQA propose a method called LoRRA, which reads the text in the image and predicts the answer which might be a deduction based on the text and the image or composed of the strings found in the image. On top of that, the aforementioned VLMs can also be potential solutions, as they have strong multimodal comprehension and generality.

Given the remarkable multimodal capabilities of VLMs, we have harnessed their potential to address the deepfake detection challenge. To take advantage of this, we formulate the deepfake detection problem as a VQA problem by asking “Is this photo real?”.

2.4 PROMPT TUNING ON FOUNDATION MODELS

Prompt tuning is a widely adopted approach to harness the power of Language Models (LMs). It can be roughly divided into two main categories, hard prompt tuning and soft prompt tuning. As for hard prompt tuning, specific tokens from a vocabulary are tuned to have LMs cater to meet users’ needs. For instance, in (Zou et al., 2023), the authors aims to find a universal suffix that can be attached to any input query, including objectionable contents, and give positive responses rather than outright refusal. (Deng et al., 2022) introduces an additional multilayer perceptron (MLP) into frozen LM and optimizes a hard prompt via reinforcement learning (RL) and reward stabilization to enhance LM performance across various tasks. (Zhang et al., 2022) employs an RL agent to adjust the initial prompts based on the given queries, thus optimizing the performance in diverse downstream tasks.

Since hard prompts are tokens from a vocabulary, it offers great interpretability and transferability to different LMs. However, the natural discreteness of these tokens also makes them hard to be optimized. Therefore, some explore another category, soft prompt tuning, where continuous word embeddings are tuned instead. As in (Chen et al., 2023), the authors optimize a soft prompt to guide an open-source LLM to generate instructions for black-box LLM, resulting in improved performance for the latter. (Li & Liang, 2021; Liu et al., 2023b) optimizes several word embeddings appended or prepended to the original prompts for different downstream tasks and outperforms their alternative in small-dataset settings. (Lester et al., 2021; Hambardzumyan et al., 2021) demonstrates how soft prompt tuning offers a simple yet effective way to condition a frozen model (especially the one with over billions of parameters), and further shows its benefits in robustness to domain transfer.

Inspired by these findings, prompt tuning for text-to-image generative models, including GAN-based models and diffusion-based models, allows generative models to receive prompts that can better convey user-provided concepts and thus improves the alignments between generated images and the input prompts (Wen et al., 2023; Gal et al., 2022; Ruiz et al., 2022). These approaches enable users to “personalize” generative models to meet their needs. In this paper, we apply textual inversion atop InstructBLIP in order to optimize an instruction that can more accurately describe the idea of differentiating real and fake images, resulting in better performance of our detector, AntifakePrompt.

³<https://chat.openai.com/>

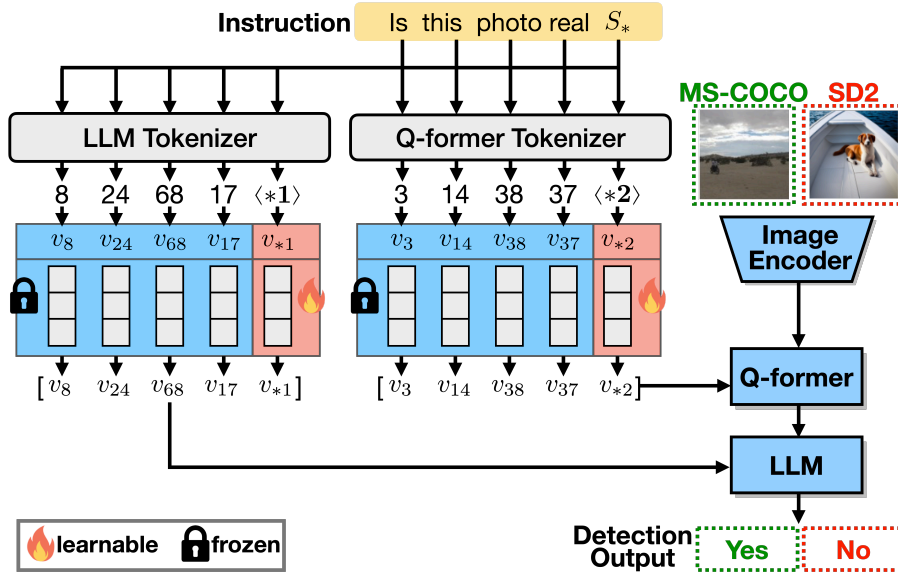


Figure 1: **Prompt tuning on InstructBLIP (Dai et al., 2023) for deepfake detector training.** An instruction containing a pseudo-word S_* is first converted into tokens. These tokens are converted to continuous vector representations (the “embeddings”, v). Then, the embedding vectors are fed into Q-former and LLM with the image features extracted by the image encoder. Finally, the embedding vectors v_{*1} and v_{*2} are optimized using language modeling loss, expecting the output to be “Yes” for real images and “No” for fake images.

3 ANTIFAKEPROMPT

3.1 PROBLEM FORMULATION

In order to take advantage of the vision-language model, we formulate the deepfake detection problem as a visual question answering (VQA) problem. In this framework, the input consists of a query image \mathbf{I} that needs to be classified as real or fake and a question prompt q . The prompt can be either a preset question (e.g., “Is this photo real?”) or a tunable question that includes the pseudo-word S_* . The output of this framework corresponds to the answer texts y . While y in principle can be any texts, we constrain it to two options: “Yes” and “No” during testing, aligning with the answer ground truth to the original binary classification problem. We choose the option with a higher probability from the VLM as the answer, and the model capability is evaluated by classification accuracy.

In summary, the deepfake detection task can be formulate as a VQA task, which is defined as:

$$\mathcal{M}(\mathbf{I}, q) \mapsto y \quad (1)$$

where \mathcal{M} is an VLM and we adopt InstructBLIP (the recent state-of-the-art) for building our method, and the text output $y \in \{\text{“Yes”}, \text{“No”}\}$ corresponds to the binary results of deepfake detection.

3.2 PROMPT TUNING ON INSTRUCTBLIP

As discussed in (Dai et al., 2023), the prompt plays an essential role in VQA problem, and asking the preset question leads to ineffective performance on unseen data. Therefore, we employ soft prompt tuning on InstructBLIP (Dai et al., 2023) following the procedure below.

Within InstructBLIP, two components receive the prompt as input: Q-Former and the Large Language Model (LLM). As shown in Figure 1, the prompt first gets tokenized and embedded, and it is then fed into Q-Former and the LLM in parallel. We introduce a pseudo-word S_* into the prompt, which serves as the target for soft prompt tuning. Specifically, we adopt the question template, “Is this photo real?” and append the pseudo-word to the end of the prompt, resulting in the modified prompt q_* : “Is this photo real S_* ?”. As the prompt has been decided, we give the output label $\hat{y} = \text{“Yes”}$ for real images and $\hat{y} = \text{“No”}$ for fake images in order to perform soft prompt tuning.

We freeze all the modules of the model except for the word embedding v_* of the pseudo-word S_* , which is randomly initialized. Then we optimize the word embedding v_* of the pseudo-word over a training set of triplet $\{\mathbf{I}, q_*, \hat{y}\}$ with respect to the language modeling loss, expecting the VLM output y to be the label \hat{y} . Hence, our optimization goal can be defined as:

$$\tilde{S}_* = \arg \min_{S_*} \mathbb{E}_{(\mathbf{I}, \hat{y})} \mathcal{L}(\mathcal{M}(\mathbf{I}, \text{“Is this image real } S_*\text{”}), \hat{y}) \quad (2)$$

where \mathcal{L} is the language modeling loss function. Since we actually optimize the embedding v_* for the pseudo-word S_* , with noting the concatenation of embeddings for the original prompt (i.e. “Is this photo real”) to be v_p , the equation can be rewritten as:

$$\tilde{v}_* = \arg \min_{v_*} \mathbb{E}_{(\mathbf{I}, \hat{y})} \mathcal{L}(\mathcal{M}(\mathbf{I}, [v_p, v_*]), \hat{y}) \quad (3)$$

As Figure 1 shows, it is crucial to highlight that the pseudo-word embedding fed into Q-Former v_{*1} differs from that fed into the LLM v_{*2} , and we optimize these two embeddings simultaneously. The dimensions of v_{*1} and v_{*2} are 768 and 4096 respectively, so the number of trainable parameters is 4864 in total. Compared to 23 million trainable parameters from ResNet-50 (He et al., 2016) of (Wang et al., 2020) and 11 million trainable parameters from ResNet-18 (He et al., 2016) of DE-FAKE (Sha et al., 2022), our method demonstrates superior cost-efficiency.

Implementation details. We use the LAVIS library⁴ for implementation, training, and evaluation. To avoid the out-of-memory issue on small GPUs, we choose Vicuna-7B (Chiang et al., 2023) as our LLM. During prompt tuning, we initialize the model from instruction-tuned checkpoint provided by LAVIS, and only finetune the word embeddings of the pseudo-word while keeping all the other parts of the model frozen. All models are prompt-tuned with a maximum of 10 epochs. We use AdamW (Loshchilov & Hutter, 2017) optimizer with $\beta_1 = 0.9$ and $\beta_2 = 0.999$, batch size 6 and a weight decay 0.05. We initially set the learning rate to 10^{-8} , and apply a cosine decay with a minimum learning rate of 0. All models are trained utilizing 4 NVIDIA RTX 3090 GPUs and completed within 10 hours. In terms of image preprocessing, all images are initially resized to have a length of 224 pixels on the shorter side while maintaining original aspect ratio. During the training phase, random cropping is applied to achieve a final size of 224×224 pixels, while images are center cropped to a final size of 224×224 pixels in the testing phase.

4 EXPERIMENTS

4.1 SETUP

Datasets We use Microsoft COCO (MS COCO) (Lin et al., 2014) dataset and Flickr30k (Young et al., 2014) dataset. Being widely utilized as benchmarks of object detection and captioning task, these datasets offer a diverse collection of images depicting people or objects engaged in everyday scenarios, and each of the images is associated with informative caption ground truth. In our work, we selected 90K images, with shorter sides greater than 224, from MS COCO dataset to train our deepfake detector. Moreover, to assess the generalizability of our method over various real images, we additionally select 3K images from Flickr30k dataset to form a held-out testing dataset, adhering to the same criterion of image size.

Generation tasks and generative models In order to evaluate the generalizability and robustness of our model to fake images from emerging and unseen generators, our testing datasets include fake images using 11 different generative models and 3 distinct attack scenarios. Here, we divide these images into six categories.

1. **Text-to-images generation:** We collected 3K prompts, half of which are sampled from the MS COCO ground truth captions and the other half from Flickr30k captions. These prompts are then input into five different generative models, i.e. SD2 (Rombach et al., 2022), SDXL (Podell et al., 2023), DeepFloyd IF (StabilityAI, 2023), DALLE-2 (Ramesh et al., 2022), and SGXL (Sauer et al., 2022a), to generate the corresponding images.

⁴<https://github.com/salesforce/LAVIS>

2. **Image stylization:** We begin by extracting Canny edge features from the 3000 test images in MS COCO dataset mentioned in the previous paragraph. Subsequently, we pass these Canny edge feature images, along with the corresponding prompts, into ControlNet (Zhang & Agrawala, 2023) to generate stylized images.
3. **Image inpainting:** We employ the same 3000 test images and resize them to make the shorter side of each image be 224, which matches the input size of InstructBLIP. Then, we randomly generate masks of three distinct thickness levels for these resized images using the scripts from the LaMa (Suvorov et al., 2022) GitHub⁵. With original images and the corresponding masks prepared, we utilize two different models, SD2-Inpainting (SD2IP) and LaMa, to inpaint images, respectively. The resizing step ensures that most of artifacts created during the inpainting process will be retained before being inputted to the detector.
4. **Super Resolution:** Out of the same reason in the inpainting, we apply the same resizing process to the same 3000 test images before downsizing them to one-fourth of their original size. These low-resolution images are then passed into two different models, SD2-SuperResolution (SD2SR) and LTE (Lee & Jin, 2022), to upsize back. A scaling factor of four is chosen, as only the $\times 4$ -upsampling weights for SD2 are publicly available.
5. **Deeperforensics:** We employ a large-scale video dataset called Deeperforensics (Jiang et al., 2020), which contains face-swapping images generated using a many-to-many end-to-end method, DF-VAE (Jiang et al., 2020). From this dataset, we randomly extract three frames from each of the 1000 generated videos without any perturbation. Following (Wang et al., 2020), we then apply Faced (Itzcovich, 2018) to crop out the faces in the extracted frames to ensure that complete facial features are present in every image.
6. **Image attacks:** We apply three common types of attacks to edit images and target at a traditional ResNet-50 classifier. The attack types include adversarial attack (Kim, 2020), backdoor attack (Li et al., 2021) and data poisoning attack (Geiping et al., 2020). Default settings are employed for each attack. By testing our detector on these attacks, we can have a better understanding of its sensitivity against these slight and malicious image editing.

It is important to note that for the fake images in the training dataset, we only include images generated by SD2 and SD2IP. Empirical evidence demonstrates that AntifakePrompt, trained solely on these two fake datasets and the real images from MS COCO dataset, exhibits excellent performance on all the other datasets generated by held-out generative models.

Baselines We compare AntifakePrompt to five recent baseline models, **Wang-2020** (Wang et al., 2020), **DE-FAKE** (Sha et al., 2022), **DIRE** (Wang et al., 2023), **InstructBLIP** (Dai et al., 2023) and **InstructBLIP with LoRA tuning** (Hu et al., 2021). For Wang-2020, we use the detector checkpoint that is trained on dataset with images that are possibly Gaussian blurr- and JPEG-augmented, each with 10% probability. For DE-FAKE, we use the checkpoint of the hybrid detector, which considers both the image and the corresponding prompts during detection. For DIRE, we use the checkpoint of detector trained on LSUN-Bedroom (Yu et al., 2015) and their corresponding generated images using StyleGAN (Karras et al., 2019). For InstructBLIP, we use the preset question prompt without prompt tuning. For InstructBLIP with LoRA, we also use the preset question prompt but applying LoRA tuning on LLM of InstructBLIP at the instruction tuning stage.

4.2 COMPARISONS

AntifakePrompt vs. different detectors. As shown in the first row of Table 1, the detector proposed by (Wang et al., 2020), trained on images generated by ProGAN (Karras et al., 2017) and ImageNet (Deng et al., 2009), exhibits satisfactory performance on SGXL and yields excellent accuracies on MS COCO and Flickr30k. However, we observe notable decreases in accuracy when it is tested on other held-out datasets. Since they consist of images generated by non-GAN-based models and these images do not share the same artifacts as those in ProGAN-generated images, the detector proposed by (Wang et al., 2020) is unable to differentiate such images by the traits learned from ProGAN-generated images.

⁵https://github.com/advimman/lama/blob/main/bin/gen_mask_dataset.py

Table 1: **Held-in and held-out deepfake detection accuracies.** Experiments are conducted on 2 real and 14 fake datasets, including 3 attacked ones. The accuracies of real and fake out-of-domain datasets are highlighted in **green** and **red**, respectively, and average accuracies are highlighted in **blue**. The accuracies of real and fake in-domain datasets are in **grey** with **lighter green** and **lighter red** background color. The best performances are denoted in **bold**. We mark the training set of InstructBLIP to be “-” to indicate that we use the pretrained model(Dai et al., 2023) without additional training set.

Methods	Training set	No. of param.	MS COCO	Flickr	SD2	SDXL	IF	DALLE-2
Wange-2020	ImageNet vs. ProGAN	23.51M	96.87	96.67	0.17	0.17	19.17	3.40
DE-FAKE	MS COCO vs. SD2	308.02M	85.97	90.67	97.10	90.50	99.20	68.97
DIRE	LSUN Bedroom vs. StyleGAN	23.51M	81.77	77.53	3.83	18.17	6.93	2.13
InstructBLIP	-	188.84M	98.93	99.63	40.27	23.07	20.63	41.77
InstructBLIP + LoRA	MS COCO vs. SD2	4.19M	95.73	91.83	98.03	96.33	86.60	99.57
AntifakePrompt	MS COCO vs. SD2	4.86K	95.37	91.00	97.83	97.27	89.73	99.57
	MS COCO vs. SD2+LaMa	4.86K	90.83	81.04	97.10	97.10	88.37	99.07
Methods	Training set	No. of param.	SGXL	ControlNet	LaMa	Inpainting SD2	Super Res. LTE	SD2
Wange-2020	ImageNet vs. ProGAN	23.51M	79.30	11.43	7.53	0.17	15.27	1.40
DE-FAKE	MS COCO vs. SD2	308.02M	56.90	63.97	13.03	16.00	9.97	29.70
DIRE	LSUN Bedroom vs. StyleGAN	23.51M	45.27	9.90	13.23	11.37	12.53	2.77
InstructBLIP	-	188.84M	69.53	33.97	10.90	44.23	97.23	69.10
InstructBLIP + LoRA	MS COCO vs. SD2	4.19M	97.67	92.87	59.50	93.03	99.53	99.97
AntifakePrompt	MS COCO vs. SD2	4.86K	99.97	91.47	39.03	85.20	99.90	99.93
	MS COCO vs. SD2+LaMa	4.86K	99.93	93.27	58.53	90.70	100.00	99.97
Methods	Training set	No. of param.	Deeper-Forensics	Adver.	Attack Backdoor	Data Poisoning	Average	
Wange-2020	ImageNet vs. ProGAN	23.51M	0.30	4.93	15.50	0.97	22.08	
DE-FAKE	MS COCO vs. SD2	308.02M	86.97	60.40	22.23	55.87	59.22	
DIRE	LSUN Bedroom vs. StyleGAN	23.51M	0.27	1.60	1.93	1.00	18.14	
InstructBLIP	-	188.84M	13.83	5.50	3.17	1.60	42.09	
InstructBLIP + LoRA	MS COCO vs. SD2	4.19M	98.80	64.30	53.40	50.87	86.13	
AntifakePrompt	MS COCO vs. SD2	4.86K	97.90	96.70	93.00	91.57	91.59	
	MS COCO vs. SD2+LaMa	4.86K	97.77	97.20	97.10	93.63	92.60	

Regarding the detector proposed in DE-FAKE (Sha et al., 2022), trained on images generated by SD and MS COCO, it demonstrates impressive performance on MS COCO, Flickr30k, 3 diffusion-based models (i.e. SD2, SDXL, and IF) and Deeperforensics, as shown in the second row of Table 1. However, it struggles to achieve accuracies above 70% on other held-out datasets.

Because the detector proposed in DE-FAKE (Sha et al., 2022) uses a similar backbone as that in (Wang et al., 2020), it suffers from similar accuracy drops when applying to images generated by unseen generative models. Even though it takes the corresponding prompts into consideration, which allows it to detect unusual scenarios of fake images, it still fails to improve its performance on held-out datasets, since most of them are generated by natural prompts from MS COCO dataset.

As for the detector proposed in (Wang et al., 2023), which employs ResNet-50 backbone trained on images generated by the prompt “A photo of bedroom” using ADM (Dhariwal & Nichol, 2021) and those from LSUN-bedroom (Yu et al., 2015), it only captures limited artifacts of a small range of data. Therefore, it suffers from severe performance drops when testing on images generated by various prompts using different generative models.

AntifakePrompt vs. different tuning methods. Furthermore, we conduct extended experiments to compare among InstructBLIP without prompt tuning, LoRA-based (Hu et al., 2021) InstructBLIP parameter finetuning and AntifakePrompt.

The results reveal that, as depicted in the forth row in Table 1, InstructBLIP without prompt tuning, demonstrates generally lower accuracies on most of the testing datasets. Compared to this, AntifakePrompt, trained only on images generated by SD2 and those from MS COCO dataset, exhibits excellent (>85%) performance on most held-in and held-out datasets, as depicted in the sixth row of Table 1. This implies that with the help of prompt tuning, AntifakePrompt can better understand the deepfake detection task. Thus, AntifakePrompt is capable of collecting more useful visual features from the input image, resulting in making more accurate decisions on distinguishing real images from fake ones.

Table 2: The accuracies of real and fake out-of-domain datasets are highlighted in green and red, respectively, and average accuracies are highlighted in blue. The best performances are in bold.

(a) Ablation study: Position of S_* in the tuned prompt (i.e. “prefix”, “postfix”, or “replace”).

Methods	Variant	MS COCO	Flickr	SD2	SDXL	IF	DALLE-2
AntifakePrompt	Replace	95.13	86.20	95.80	93.60	87.33	99.17
	Prefix	95.80	89.57	97.27	96.47	88.77	97.90
	Postfix	95.37	91.00	97.83	97.27	89.73	99.57

Methods	Variant	SGXL	ControlNet	Inpainting LaMa	SD2	Super Res. LTE	SD2
AntifakePrompt	Replace	98.37	99.70	33.40	78.63	99.97	99.70
	Prefix	99.87	89.43	40.33	84.67	99.97	99.87
	Postfix	99.97	91.47	39.03	85.20	99.90	99.93

Methods	Variant	Deeper- Forensics	Adver.	Attack Backdoor	Data Poisoning	Average
AntifakePrompt	Replace	93.03	90.43	86.00	86.63	88.94
	Prefix	94.17	93.53	93.13	87.43	90.51
	Postfix	97.90	96.70	93.00	91.57	91.59

(b) Ablation study: Prompt tuning for Q-former, LLM or both.

Methods	Prompt tuning for	MS COCO	Flickr	SD2	SDXL	IF	DALLE-2
AntifakePrompt	Only Q-former	93.50	92.27	97.93	98.17	88.47	99.53
	Only LLM	95.10	85.57	95.77	91.73	85.23	98.73
	Both	95.37	91.00	97.83	97.27	89.73	99.57

Methods	Prompt tuning for	SGXL	ControlNet	Inpainting LaMa	SD2	Super Res. LTE	SD2
AntifakePrompt	Only Q-former	94.80	89.33	37.67	77.50	99.93	99.67
	Only LLM	97.80	84.90	31.37	77.77	99.87	99.40
	Both	99.97	91.47	39.03	85.20	99.90	99.93

Methods	Prompt tuning for	Deeper- Forensics	Adver.	Attack Backdoor	Data Poisoning	Average
AntifakePrompt	Only Q-former	100.00	97.53	97.97	95.23	91.22
	Only LLM	93.30	86.03	83.47	83.50	86.85
	Both	97.90	96.70	93.00	91.57	91.59

Furthermore, as shown in the fifth and sixth rows in Table 1 corresponding to “AntifakePrompt” with training set “COCO vs. SD2” for our model performance to make comparison, while the detector finetuned with LoRA achieves comparable results in certain testing datasets, AntifakePrompt consistently outperforms it in the three attack datasets. This is because additional LoRA matrices introduce relatively more learnable parameters into LLM than those introduced by prompt tuning (around 4M vs. 4K), it is more likely for LoRA-tuned InstructBLIP to overfit to artifacts of training datasets, resulting in accuracy drops when applied to fake datasets with different traits, namely three attack datasets.

Also, AntifakePrompt achieves accuracies exceeding 90% on attacked datasets generated by 3 different attacking strategies while other 5 baselines, including pretrained detector, showcase accuracy drops compared to their performances on other datasets. We conclude that AntifakePrompt is more sensitive to the slight and malicious pixel perturbations than its opponents.

Additionally, to address the relatively lower performance observed on LaMa testing dataset, we conduct an experiment to include additional images generated by LaMa into our training dataset. Under this modified setting, as depicted in the sixth and seventh rows of Table 1, AntifakePrompt gives generally comparable or even higher accuracies on almost every fake dataset compared to the original setting (the detector trained on 150K training dataset), especially in LaMa, SD2IP. The detector with modified settings also achieves the highest average accuracy among all methods.

Table 3: **Ablation study: Number of training datasets**, where either the number of the real images or that of both real and fake images in the training dataset is reduced. The accuracies of real and fake out-of-domain datasets are highlighted in **green** and **red**, respectively, and average accuracies are highlighted in **blue**. The best performances are in **bold**.

Methods	No. Data	MS COCO	Flickr	SD2	SDXL	IF	DALLE-2
AntifakePrompt	90K	89.90	80.37	98.33	98.20	92.87	98.90
	120K	94.30	89.10	97.53	96.60	89.20	98.27
	150K	95.37	91.00	97.83	97.27	89.73	99.57
	180K	96.53	92.23	97.37	96.67	88.43	99.63
	15K	92.60	92.03	92.17	90.20	75.80	97.27
	1.5K	92.83	94.10	75.67	68.20	58.17	79.77
	0.15K	99.07	99.73	33.17	16.73	16.30	36.93
Methods	No. Data	SGXL	ControlNet	LaMa	Inpainting SD2	Super Res. LTE	Super Res. SD2
AntifakePrompt	90K	99.93	94.60	49.80	89.63	100.00	99.93
	120K	99.90	91.03	41.03	85.13	99.97	99.87
	150K	99.97	91.47	39.03	85.20	99.90	99.93
	180K	99.93	90.43	36.87	84.27	99.73	99.93
	15K	97.97	81.27	34.73	73.93	100.00	98.43
	1.5K	90.63	67.50	30.80	67.57	99.87	90.00
	0.15K	56.73	26.17	8.90	40.53	95.23	63.53
Methods	No. Data	Deeper-Forensics	Adver.	Attack Backdoor	Data Poisoning	Average	
AntifakePrompt	90K	99.27	98.40	96.40	94.97	92.59	
	120K	95.13	97.87	96.00	95.37	91.64	
	150K	97.90	96.70	93.00	91.57	91.59	
	180K	94.63	94.83	91.50	90.57	90.85	
	15K	91.93	84.07	82.57	74.53	84.97	
	1.5K	67.53	29.57	25.93	11.87	65.63	
	0.15K	24.20	3.97	2.40	1.43	39.06	

4.3 ABLATION STUDY

Position of S_* in the tuned prompt. Comparing the accuracies between InstructBLIP and AntifakePrompt, we empirically show how we ask questions can drastically affect the results. Here, we further investigate how the positioning of pseudo-word S_* in the the tuned prompt can influence AntifakePrompt. Specifically, we compare 3 different positions of placing pseudo-word: replacing the word “real” in the original prompt with pseudo-word, positioning the pseudo-word in the beginning of the prompt, or placing it at the end of the prompt. For simplicity, we refer to them as “replace”, “prefix” and “postfix”, respectively. As presented in Table 2a, although they all yield overall high accuracies, the “postfix” position exhibits a slight advantage over the other alternatives. This suggests placing the pseudo-word at the end of the prompt makes the best efforts among 3 different positions to enable deepfake detection, although the performance difference is not sensitive.

Prompt tuning for the Q-former, LLM or both? We extend our study to the impact of prompt tuning by comparing the results of applying prompt tuning exclusively to Q-former, LLM or both modules. In Table 2b, we observe that prompt tuning for both Q-former and LLM outperforms other two alternatives in average accuracy. This implies that prompt tuning for both modules are beneficial: tuned prompts to Q-former allow it to extract visual features from input image embeddings that are more conducive to differentiating between real and fake images. Tuned prompts to LLM can more precisely describe the idea of fake image detection for LLM, and thus, LLM is able to make more accurate decisions on differentiating real and fake images. Due to the improved visual features and the improved instruction, the application of prompt tuning for both Q-former and LLM yields better performance.

Number of training images. We first study the effect of the number of real images in the training dataset. While fixing the number of fake images in training dataset to 60K, we gradually increase the number of real images from 30K to 120K in the step of 30K, resulting in the total size of our training

dataset ranging from 90K to 180K. As shown in first to fourth rows in Table 3, while the accuracies on testing datasets of real images increase along with the increments of real images in training dataset, AntifakePrompt suffers from a decrease in accuracies on fake testing datasets. Therefore, we designate the detector trained on 150K training dataset as our optimal model, achieving balanced accuracies on real and fake images.

To explore the limit of few-shot learning ability of AntifakePrompt, we gradually reduce the numbers of both real and fake images in training dataset to one tenth at each step until only 150 images remain in total. As shown in the fifth to seventh rows in Table 3, we found out that AntifakePrompt still outperforms DE-FAKE in almost every testing datasets when there are as few as 15K training samples, almost a quarter of DE-FAKE. Additionally, when we reduce our training dataset to only 1.5K images, only 0.2% of (Wang et al., 2020) training dataset, AntifakePrompt outperforms (Wang et al., 2020) on every fake dataset, exhibiting only slightly lower accuracies on real datasets. These findings underscore the data efficiency of AntifakePrompt in terms of training data size compared to two baseline models.

5 CONCLUSION

In this paper, we propose AntifakePrompt to solve deepfake detection problem utilizing the vision-language model and address the limitations of traditional deepfake detection methods when being applied on held-out datasets. We formulate the deepfake detection problem as a visual question answering problem, and apply soft prompt tuning on InstructBLIP. Empirical results demonstrate improved performance of AntifakePrompt over both held-in and held-out testing datasets, which is trained solely on generated images using SD2 and real images from MS COCO datasets. Furthermore, in contrast to prior studies which require to finetune/learn millions of parameters, our model only needs to tune much less parameters, thus striking a better balance between the training cost and the effectiveness. Consequently, AntifakePrompt provides a potent defense against the potential risks associated with the misuse of generative models, while demanding fewer training resources.

REFERENCES

- Andrew Brock, Jeff Donahue, and Karen Simonyan. Large scale gan training for high fidelity natural image synthesis. *arXiv preprint arXiv:1809.11096*, 2018.
- Lichang Chen, Jiu-hai Chen, Tom Goldstein, Heng Huang, and Tianyi Zhou. Instructzero: Efficient instruction optimization for black-box large language models. *arXiv preprint arXiv:2306.03082*, 2023.
- Yinbo Chen, Sifei Liu, and Xiaolong Wang. Learning continuous image representation with local implicit image function. In *Proceedings of the IEEE/CVF conference on computer vision and pattern recognition*, pp. 8628–8638, 2021.
- Wei-Lin Chiang, Zhuohan Li, Zi Lin, Ying Sheng, Zhanghao Wu, Hao Zhang, Lianmin Zheng, Siyuan Zhuang, Yonghao Zhuang, Joseph E Gonzalez, et al. Vicuna: An open-source chatbot impressing gpt-4 with 90%* chatgpt quality. See <https://vicuna.lmsys.org> (accessed 14 April 2023), 2023.
- Hyung Won Chung, Le Hou, Shayne Longpre, Barret Zoph, Yi Tay, William Fedus, Eric Li, Xuezhi Wang, Mostafa Dehghani, Siddhartha Brahma, et al. Scaling instruction-finetuned language models. *arXiv preprint arXiv:2210.11416*, 2022.
- Wenliang Dai, Junnan Li, Dongxu Li, Anthony Meng Huat Tiong, Junqi Zhao, Weisheng Wang, Boyang Li, Pascale Fung, and Steven Hoi. Instructblip: Towards general-purpose vision-language models with instruction tuning, 2023.
- Jia Deng, Wei Dong, Richard Socher, Li-Jia Li, Kai Li, and Li Fei-Fei. Imagenet: A large-scale hierarchical image database. In *2009 IEEE conference on computer vision and pattern recognition*, pp. 248–255. Ieee, 2009.

- Mingkai Deng, Jianyu Wang, Cheng-Ping Hsieh, Yihan Wang, Han Guo, Tianmin Shu, Meng Song, Eric P Xing, and Zhiting Hu. Rlprompt: Optimizing discrete text prompts with reinforcement learning. *arXiv preprint arXiv:2205.12548*, 2022.
- Prafulla Dhariwal and Alexander Nichol. Diffusion models beat gans on image synthesis. In M. Ranzato, A. Beygelzimer, Y. Dauphin, P.S. Liang, and J. Wortman Vaughan (eds.), *Advances in Neural Information Processing Systems*, volume 34, pp. 8780–8794. Curran Associates, Inc., 2021. URL https://proceedings.neurips.cc/paper_files/paper/2021/file/49ad23d1ec9fa4bd8d77d02681df5cfa-Paper.pdf.
- D. C. Dowson and B. V. Landau. The fréchet distance between multivariate normal distributions. *Journal of Multivariate Analysis*, 12(3):450–455, 1982. URL <https://EconPapers.repec.org/RePEc:eee:jmvana:v:12:y:1982:i:3:p:450-455>.
- David C Epstein, Ishan Jain, Oliver Wang, and Richard Zhang. Online detection of ai-generated images. In *Proceedings of the IEEE/CVF International Conference on Computer Vision*, pp. 382–392, 2023.
- Joel Frank, Thorsten Eisenhofer, Lea Schönherr, Asja Fischer, Dorothea Kolossa, and Thorsten Holz. Leveraging frequency analysis for deep fake image recognition. In *International conference on machine learning*, pp. 3247–3258. PMLR, 2020.
- Rinon Gal, Yuval Alaluf, Yuval Atzmon, Or Patashnik, Amit H Bermano, Gal Chechik, and Daniel Cohen-Or. An image is worth one word: Personalizing text-to-image generation using textual inversion. *arXiv preprint arXiv:2208.01618*, 2022.
- Jonas Geiping, Liam Fowl, W Ronny Huang, Wojciech Czaja, Gavin Taylor, Michael Moeller, and Tom Goldstein. Witches’ brew: Industrial scale data poisoning via gradient matching. *arXiv preprint arXiv:2009.02276*, 2020.
- Oliver Giudice, Luca Guarnera, and Sebastiano Battiato. Fighting deepfakes by detecting gan dct anomalies. *Journal of Imaging*, 7(8):128, 2021.
- Ian Goodfellow, Jean Pouget-Abadie, Mehdi Mirza, Bing Xu, David Warde-Farley, Sherjil Ozair, Aaron Courville, and Yoshua Bengio. Generative adversarial nets. In Z. Ghahramani, M. Welling, C. Cortes, N. Lawrence, and K.Q. Weinberger (eds.), *Advances in Neural Information Processing Systems*, volume 27. Curran Associates, Inc., 2014.
- Yash Goyal, Tejas Khot, Douglas Summers-Stay, Dhruv Batra, and Devi Parikh. Making the v in vqa matter: Elevating the role of image understanding in visual question answering. In *Proceedings of the IEEE conference on computer vision and pattern recognition*, pp. 6904–6913, 2017.
- Luca Guarnera, Oliver Giudice, and Sebastiano Battiato. Level up the deepfake detection: a method to effectively discriminate images generated by gan architectures and diffusion models. *arXiv preprint arXiv:2303.00608*, 2023.
- Xiao Guo, Xiaohong Liu, Zhiyuan Ren, Steven Grosz, Iacopo Masi, and Xiaoming Liu. Hierarchical fine-grained image forgery detection and localization. In *Proceedings of the IEEE/CVF Conference on Computer Vision and Pattern Recognition*, pp. 3155–3165, 2023.
- Danna Gurari, Qing Li, Abigale J Stangl, Anhong Guo, Chi Lin, Kristen Grauman, Jiebo Luo, and Jeffrey P Bigham. Vizwiz grand challenge: Answering visual questions from blind people. In *Proceedings of the IEEE conference on computer vision and pattern recognition*, pp. 3608–3617, 2018.
- Karen Hambardzumyan, Hrant Khachatrian, and Jonathan May. Warp: Word-level adversarial re-programming. *arXiv preprint arXiv:2101.00121*, 2021.
- Kaiming He, Xiangyu Zhang, Shaoqing Ren, and Jian Sun. Deep residual learning for image recognition. In *Proceedings of the IEEE conference on computer vision and pattern recognition*, pp. 770–778, 2016.
- Yang He, Ning Yu, Margret Keuper, and Mario Fritz. Beyond the spectrum: Detecting deepfakes via re-synthesis. *arXiv preprint arXiv:2105.14376*, 2021.

- Jonathan Ho, Ajay Jain, and Pieter Abbeel. Denoising diffusion probabilistic models. *Advances in neural information processing systems*, 33:6840–6851, 2020.
- Edward J Hu, Yelong Shen, Phillip Wallis, Zeyuan Allen-Zhu, Yanzhi Li, Shean Wang, Lu Wang, and Weizhu Chen. Lora: Low-rank adaptation of large language models. *arXiv preprint arXiv:2106.09685*, 2021.
- Ivan Itzcovich. Faced, 2018. <https://github.com/iitzco/faced>.
- Liming Jiang, Ren Li, Wayne Wu, Chen Qian, and Chen Change Loy. Deepforensics-1.0: A large-scale dataset for real-world face forgery detection. In *Proceedings of the IEEE/CVF conference on computer vision and pattern recognition*, pp. 2889–2898, 2020.
- Tero Karras, Timo Aila, Samuli Laine, and Jaakko Lehtinen. Progressive growing of gans for improved quality, stability, and variation. *arXiv preprint arXiv:1710.10196*, 2017.
- Tero Karras, Samuli Laine, and Timo Aila. A style-based generator architecture for generative adversarial networks. In *Proceedings of the IEEE/CVF conference on computer vision and pattern recognition*, pp. 4401–4410, 2019.
- Tero Karras, Samuli Laine, Miika Aittala, Janne Hellsten, Jaakko Lehtinen, and Timo Aila. Analyzing and improving the image quality of stylegan. In *Proceedings of the IEEE/CVF conference on computer vision and pattern recognition*, pp. 8110–8119, 2020.
- Tero Karras, Miika Aittala, Samuli Laine, Erik Härkönen, Janne Hellsten, Jaakko Lehtinen, and Timo Aila. Alias-free generative adversarial networks. In *Proc. NeurIPS*, 2021.
- Hoki Kim. Torchattacks: A pytorch repository for adversarial attacks. *arXiv preprint arXiv:2010.01950*, 2020.
- Jaewon Lee and Kyong Hwan Jin. Local texture estimator for implicit representation function. In *Proceedings of the IEEE/CVF conference on computer vision and pattern recognition*, pp. 1929–1938, 2022.
- Brian Lester, Rami Al-Rfou, and Noah Constant. The power of scale for parameter-efficient prompt tuning. *arXiv preprint arXiv:2104.08691*, 2021.
- Junnan Li, Dongxu Li, Caiming Xiong, and Steven Hoi. Blip: Bootstrapping language-image pre-training for unified vision-language understanding and generation. In *International Conference on Machine Learning*, pp. 12888–12900. PMLR, 2022.
- Junnan Li, Dongxu Li, Silvio Savarese, and Steven Hoi. Blip-2: Bootstrapping language-image pre-training with frozen image encoders and large language models. *arXiv preprint arXiv:2301.12597*, 2023.
- Xiang Lisa Li and Percy Liang. Prefix-tuning: Optimizing continuous prompts for generation. *arXiv preprint arXiv:2101.00190*, 2021.
- Yuezun Li, Yiming Li, Baoyuan Wu, Longkang Li, Ran He, and Siwei Lyu. Invisible backdoor attack with sample-specific triggers. In *Proceedings of the IEEE/CVF international conference on computer vision*, pp. 16463–16472, 2021.
- Tsung-Yi Lin, Michael Maire, Serge Belongie, James Hays, Pietro Perona, Deva Ramanan, Piotr Dollár, and C Lawrence Zitnick. Microsoft coco: Common objects in context. In *Computer Vision—ECCV 2014: 13th European Conference, Zurich, Switzerland, September 6–12, 2014, Proceedings, Part V 13*, pp. 740–755. Springer, 2014.
- Bo Liu, Fan Yang, Xiuli Bi, Bin Xiao, Weisheng Li, and Xinbo Gao. Detecting generated images by real images. In *European Conference on Computer Vision*, pp. 95–110. Springer, 2022.
- Haotian Liu, Chunyuan Li, Qingyang Wu, and Yong Jae Lee. Visual instruction tuning. *arXiv preprint arXiv:2304.08485*, 2023a.

- Hongyu Liu, Bin Jiang, Yibing Song, Wei Huang, and Chao Yang. Rethinking image inpainting via a mutual encoder-decoder with feature equalizations. In *Computer Vision–ECCV 2020: 16th European Conference, Glasgow, UK, August 23–28, 2020, Proceedings, Part II 16*, pp. 725–741. Springer, 2020.
- Xiao Liu, Yanan Zheng, Zhengxiao Du, Ming Ding, Yujie Qian, Zhilin Yang, and Jie Tang. Gpt understands, too. *AI Open*, 2023b.
- Ilya Loshchilov and Frank Hutter. Decoupled weight decay regularization. *arXiv preprint arXiv:1711.05101*, 2017.
- Kenneth Marino, Mohammad Rastegari, Ali Farhadi, and Roozbeh Mottaghi. Ok-vqa: A visual question answering benchmark requiring external knowledge. In *Proceedings of the IEEE/cvf conference on computer vision and pattern recognition*, pp. 3195–3204, 2019.
- Anand Mishra, Shashank Shekhar, Ajeet Kumar Singh, and Anirban Chakraborty. Ocr-vqa: Visual question answering by reading text in images. In *2019 international conference on document analysis and recognition (ICDAR)*, pp. 947–952. IEEE, 2019.
- Lakshmanan Nataraj, Tajuddin Manhar Mohammed, Shivkumar Chandrasekaran, Arjuna Flenner, Jawadul H Bappy, Amit K Roy-Chowdhury, and BS Manjunath. Detecting gan generated fake images using co-occurrence matrices. *arXiv preprint arXiv:1903.06836*, 2019.
- OpenAI. GPT-4 Technical Report. *arXiv e-prints*, art. arXiv:2303.08774, March 2023. doi: 10.48550/arXiv.2303.08774.
- OpenAI. Dalle-3, 2023. <https://openai.com/dall-e-3>.
- Dustin Podell, Zion English, Kyle Lacey, Andreas Blattmann, Tim Dockhorn, Jonas Müller, Joe Penna, and Robin Rombach. Sdxl: improving latent diffusion models for high-resolution image synthesis. *arXiv preprint arXiv:2307.01952*, 2023.
- Aditya Ramesh, Prafulla Dhariwal, Alex Nichol, Casey Chu, and Mark Chen. Hierarchical text-conditional image generation with clip latents. *arXiv preprint arXiv:2204.06125*, 1(2):3, 2022.
- Jonas Ricker, Simon Damm, Thorsten Holz, and Asja Fischer. Towards the detection of diffusion model deepfakes. *arXiv preprint arXiv:2210.14571*, 2022.
- Robin Rombach, Andreas Blattmann, Dominik Lorenz, Patrick Esser, and Björn Ommer. High-resolution image synthesis with latent diffusion models, 2021.
- Robin Rombach, Andreas Blattmann, Dominik Lorenz, Patrick Esser, and Björn Ommer. High-resolution image synthesis with latent diffusion models. In *Proceedings of the IEEE/CVF conference on computer vision and pattern recognition*, pp. 10684–10695, 2022.
- Nataniel Ruiz, Yuanzhen Li, Varun Jampani, Yael Pritch, Michael Rubinstein, and Kfir Aberman. Dreambooth: Fine tuning text-to-image diffusion models for subject-driven generation. 2022.
- Chitwan Saharia, William Chan, Saurabh Saxena, Lala Li, Jay Whang, Emily L Denton, Kamyar Ghasemipour, Raphael Gontijo Lopes, Burcu Karagol Ayan, Tim Salimans, et al. Photorealistic text-to-image diffusion models with deep language understanding. *Advances in Neural Information Processing Systems*, 35:36479–36494, 2022.
- Tim Salimans, Ian Goodfellow, Wojciech Zaremba, Vicki Cheung, Alec Radford, and Xi Chen. Improved techniques for training gans. *Advances in neural information processing systems*, 29, 2016.
- Axel Sauer, Kashyap Chitta, Jens Müller, and Andreas Geiger. Projected gans converge faster. In *Advances in Neural Information Processing Systems (NeurIPS)*, 2021.
- Axel Sauer, Katja Schwarz, and Andreas Geiger. Stylegan-xl: Scaling stylegan to large diverse datasets. In *ACM SIGGRAPH 2022 conference proceedings*, pp. 1–10, 2022a.
- Axel Sauer, Katja Schwarz, and Andreas Geiger. Stylegan-xl: Scaling stylegan to large diverse datasets. volume abs/2201.00273, 2022b. URL <https://arxiv.org/abs/2201.00273>.

- Dustin Schwenk, Apoorv Khandelwal, Christopher Clark, Kenneth Marino, and Roozbeh Mottaghi. A-okvqa: A benchmark for visual question answering using world knowledge. In *European Conference on Computer Vision*, pp. 146–162. Springer, 2022.
- Zeyang Sha, Zheng Li, Ning Yu, and Yang Zhang. De-fake: Detection and attribution of fake images generated by text-to-image diffusion models. *arXiv preprint arXiv:2210.06998*, 2022.
- Amanpreet Singh, Vivek Natarajan, Meet Shah, Yu Jiang, Xinlei Chen, Dhruv Batra, Devi Parikh, and Marcus Rohrbach. Towards vqa models that can read. In *Proceedings of the IEEE/CVF conference on computer vision and pattern recognition*, pp. 8317–8326, 2019.
- Jiaming Song, Chenlin Meng, and Stefano Ermon. Denoising diffusion implicit models. *arXiv preprint arXiv:2010.02502*, 2020.
- StabilityAI. Deepfloyd if, 2023. <https://github.com/deep-floyd/IF>.
- Roman Suvorov, Elizaveta Logacheva, Anton Mashikhin, Anastasia Remizova, Arsenii Ashukha, Aleksei Silvestrov, Naejin Kong, Harshith Goka, Kiwoong Park, and Victor Lempitsky. Resolution-robust large mask inpainting with fourier convolutions. In *Proceedings of the IEEE/CVF winter conference on applications of computer vision*, pp. 2149–2159, 2022.
- Hugo Touvron, Thibaut Lavril, Gautier Izacard, Xavier Martinet, Marie-Anne Lachaux, Timothée Lacroix, Baptiste Rozière, Naman Goyal, Eric Hambro, Faisal Azhar, et al. Llama: Open and efficient foundation language models. *arXiv preprint arXiv:2302.13971*, 2023.
- Sheng-Yu Wang, Oliver Wang, Richard Zhang, Andrew Owens, and Alexei A Efros. Cnn-generated images are surprisingly easy to spot... for now. In *IEEE Conference on Computer Vision and Pattern Recognition (CVPR)*, pp. 8695–8704, 2020.
- Zhendong Wang, Jianmin Bao, Wengang Zhou, Weilun Wang, Hezhen Hu, Hong Chen, and Houqiang Li. Dire for diffusion-generated image detection. *arXiv preprint arXiv:2303.09295*, 2023.
- Yuxin Wen, Neel Jain, John Kirchenbauer, Micah Goldblum, Jonas Geiping, and Tom Goldstein. Hard prompts made easy: Gradient-based discrete optimization for prompt tuning and discovery. *arXiv preprint arXiv:2302.03668*, 2023.
- Qinghao Ye, Haiyang Xu, Guohai Xu, Jiabo Ye, Ming Yan, Yiyang Zhou, Junyang Wang, Anwen Hu, Pengcheng Shi, Yaya Shi, et al. mplug-owl: Modularization empowers large language models with multimodality. *arXiv preprint arXiv:2304.14178*, 2023.
- Peter Young, Alice Lai, Micah Hodosh, and Julia Hockenmaier. From image descriptions to visual denotations: New similarity metrics for semantic inference over event descriptions. *Transactions of the Association for Computational Linguistics*, 2:67–78, 2014.
- Fisher Yu, Ari Seff, Yinda Zhang, Shuran Song, Thomas Funkhouser, and Jianxiong Xiao. Lsun: Construction of a large-scale image dataset using deep learning with humans in the loop. *arXiv preprint arXiv:1506.03365*, 2015.
- Ning Yu, Larry S Davis, and Mario Fritz. Attributing fake images to gans: Learning and analyzing gan fingerprints. In *Proceedings of the IEEE/CVF international conference on computer vision*, pp. 7556–7566, 2019.
- Sangdoon Yun, Dongyoon Han, Seong Joon Oh, Sanghyuk Chun, Junsuk Choe, and Youngjoon Yoo. Cutmix: Regularization strategy to train strong classifiers with localizable features. In *Proceedings of the IEEE/CVF international conference on computer vision*, pp. 6023–6032, 2019.
- Han Zhang, Ian Goodfellow, Dimitris Metaxas, and Augustus Odena. Self-attention generative adversarial networks. In *International conference on machine learning*, pp. 7354–7363. PMLR, 2019a.
- Lvmin Zhang and Maneesh Agrawala. Adding conditional control to text-to-image diffusion models. *arXiv preprint arXiv:2302.05543*, 2023.

- Tianjun Zhang, Xuezhi Wang, Denny Zhou, Dale Schuurmans, and Joseph E Gonzalez. Tempera: Test-time prompt editing via reinforcement learning. In *The Eleventh International Conference on Learning Representations*, 2022.
- Xu Zhang, Svebor Karaman, and Shih-Fu Chang. Detecting and simulating artifacts in gan fake images. In *2019 IEEE international workshop on information forensics and security (WIFS)*, pp. 1–6. IEEE, 2019b.
- Deyao Zhu, Jun Chen, Xiaoqian Shen, Xiang Li, and Mohamed Elhoseiny. Minigt-4: Enhancing vision-language understanding with advanced large language models. *arXiv preprint arXiv:2304.10592*, 2023.
- Andy Zou, Zifan Wang, J Zico Kolter, and Matt Fredrikson. Universal and transferable adversarial attacks on aligned language models. *arXiv preprint arXiv:2307.15043*, 2023.

A SAMPLES FOR EACH DATASETS

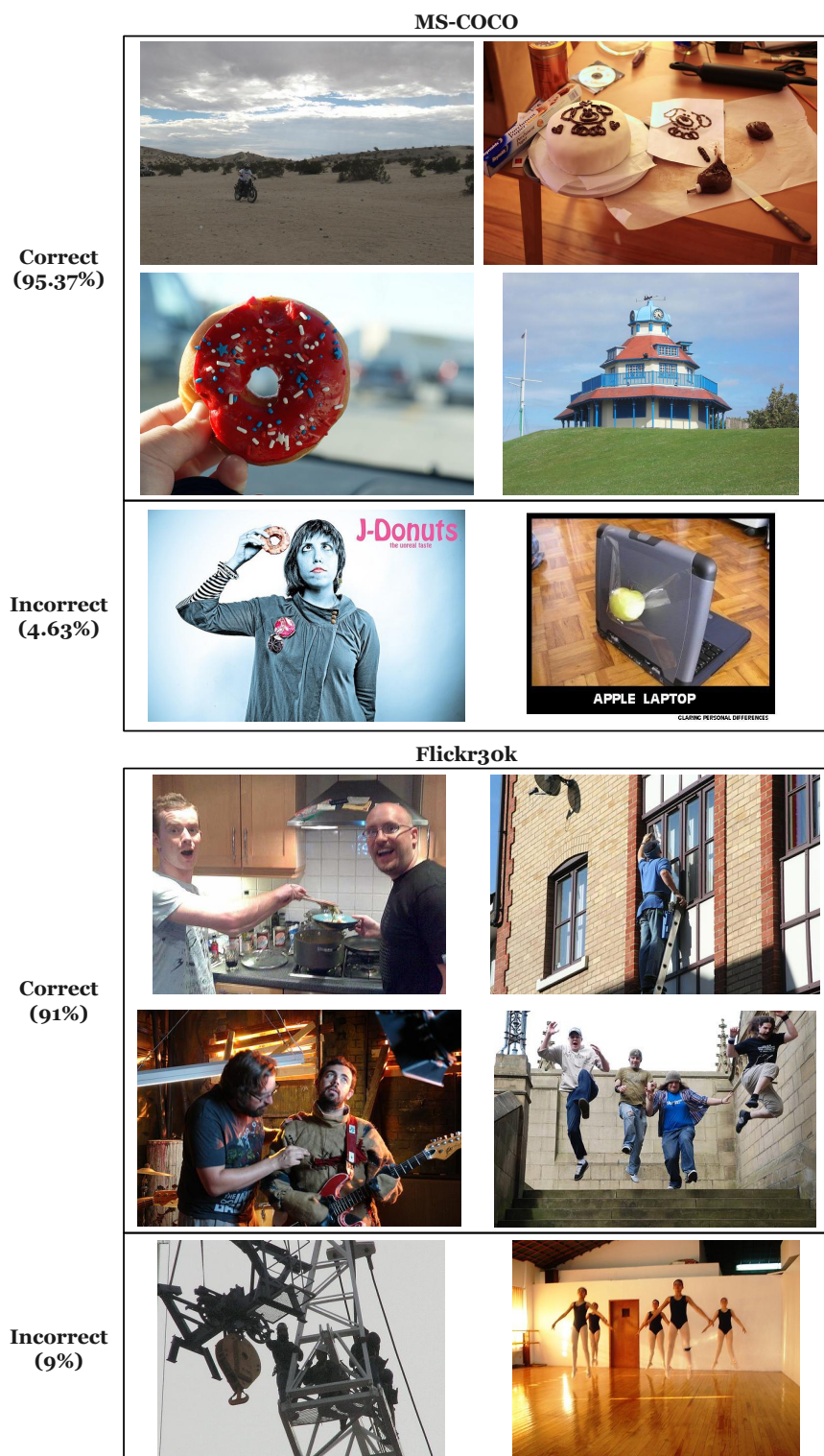


Figure 2: **Samples for each datasets.** 95.37% / 91% of images in MS-COCO / Flickr30k are correctly classified as real.

SD2

Correct
(97.83%)

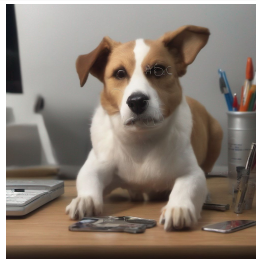
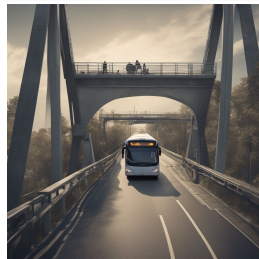


Incorrect
(2.17%)



SDXL

Correct
(97.27%)



Incorrect
(2.73%)

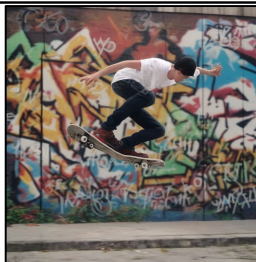
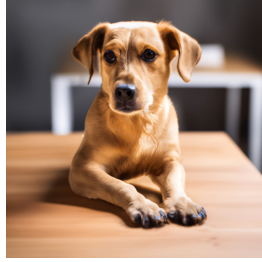


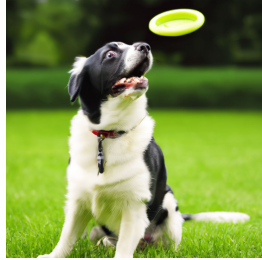
Figure 3: **Samples for each datasets (Continue).** 97.83% / 97.27% of images generated by SD2 / SDXL are correctly classified as real / fake.

IF

Correct
(89.73%)



Incorrect
(10.27%)



DALLE-2

Correct
(99.57%)



Incorrect
(0.43%)

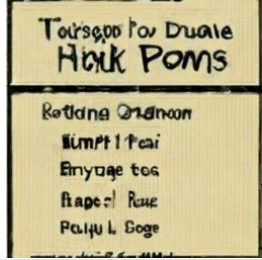


Figure 4: Samples for each datasets (Continue). 89.73% / 99.57% of images generated by IF / DALLE-2 are correctly classified as fake.

SGXL

Correct
(99.97%)



Incorrect
(0.03%)



ControlNet

Correct
(91.47%)



Incorrect
(8.53%)



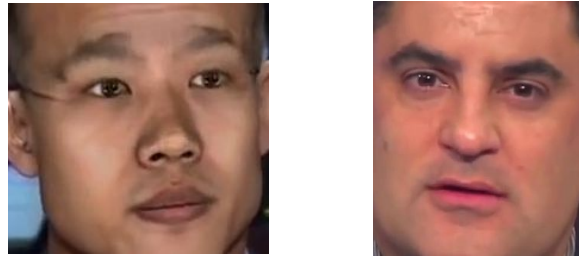
Figure 5: **Samples for each datasets (Continue).** 99.97% / 91.47% of images generated by SGXL / ControlNet are correctly classified as fake.

Deeperforensics

**Correct
(97.9%)**

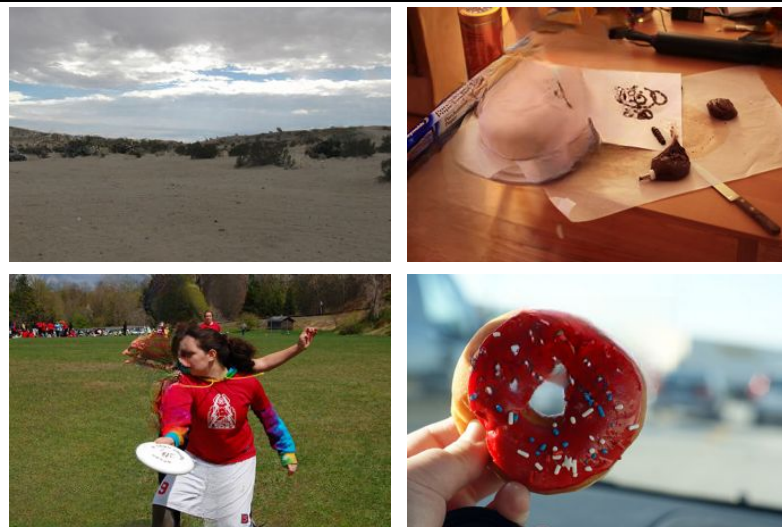


**Incorrect
(2.1%)**



LaMa

**Correct
(39.03%)**



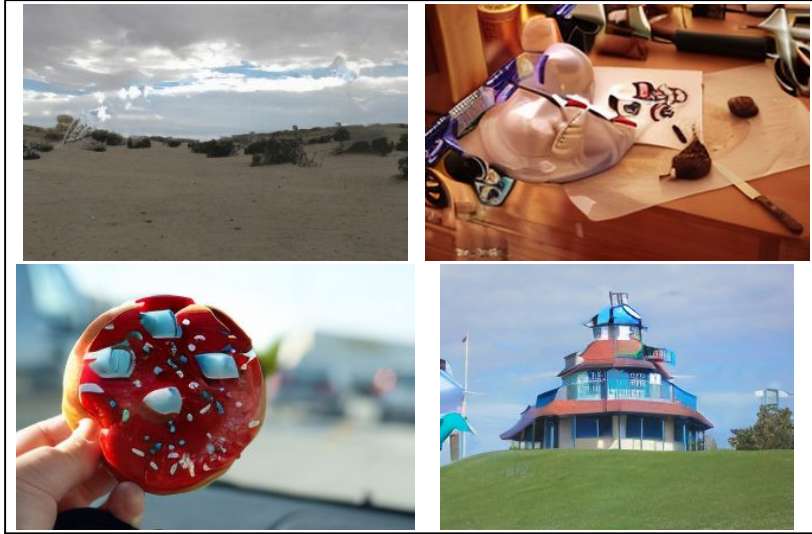
**Incorrect
(60.97%)**



Figure 6: **Samples for each datasets (Continue).** 97.9% / 39.03% of images in Deeperforensics / generated by LaMa are correctly classified as fake.

SD2IP

**Correct
(85.2%)**

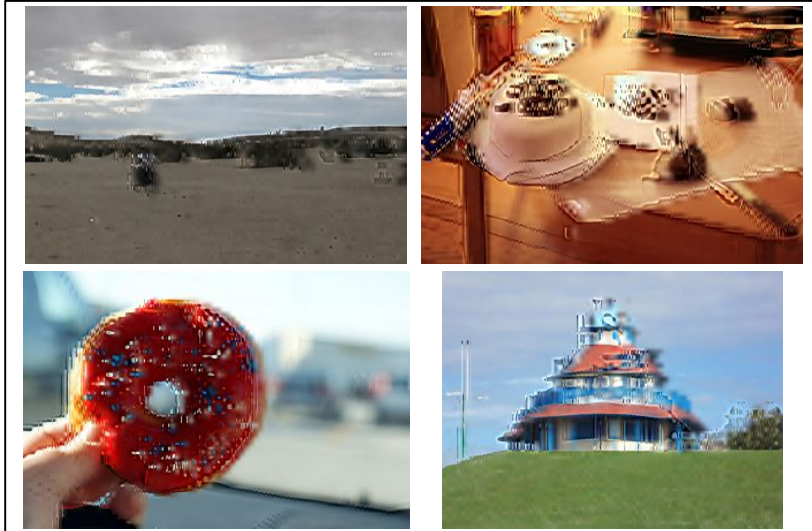


**Incorrect
(14.8%)**



LTE

**Correct
(99.9%)**



**Incorrect
(0.1%)**



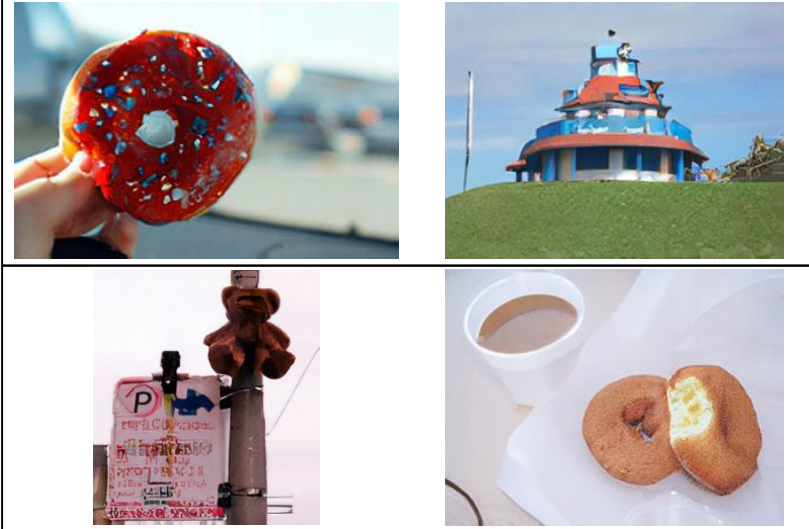
Figure 7: **Samples for each datasets (Continue)**. 85.2% / 99.9% of images generated by SD2IP / LTE are correctly classified as fake.

SD2SR

Correct
(99.93%)

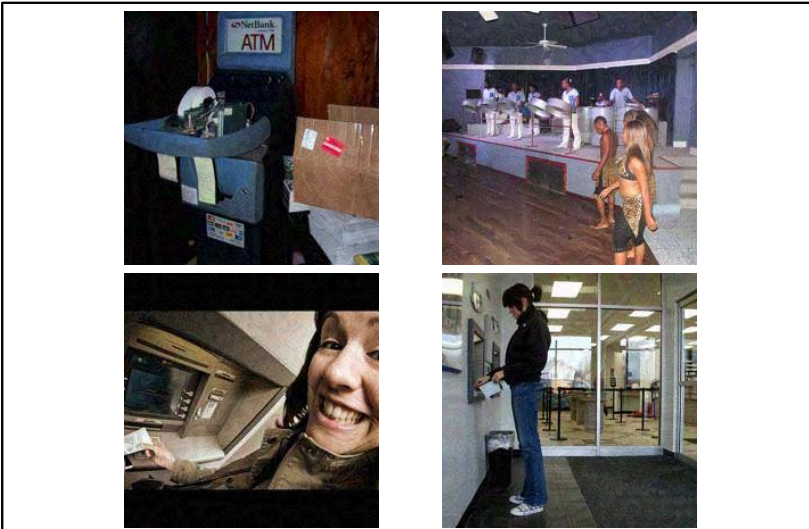


Incorrect
(0.07%)



Adversarial Attack

Correct
(96.7%)



Incorrect
(3.3%)

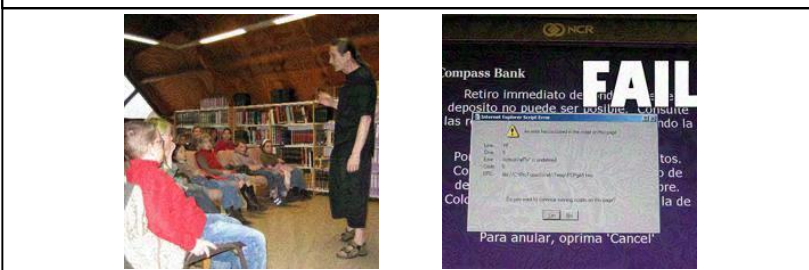


Figure 8: **Samples for each datasets (Continue).** 99.93% / 96.7% of images generated by SD2SR / under adversarial attack are correctly classified as fake.

Backdoor Attack

Correct
(93%)

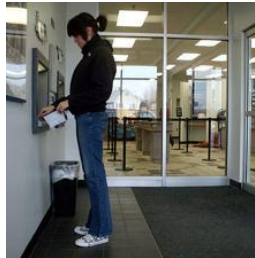


Incorrect
(7%)



Data Poison Attack

Correct
(91.57%)



Incorrect
(8.43%)



Figure 9: **Samples for each datasets (Continue).** 93% / 91.57% of images generated under backdoor / data poison attack are correctly classified as fake.